

TIMELY UPDATING WITH INTERMITTENT ENERGY AND DATA FOR  
MULTIPLE SOURCES OVER ERASURE CHANNELS

by

Christopher Daniel Jr.

A thesis submitted to the faculty of  
The University of North Carolina at Charlotte  
in partial fulfillment of the requirements  
for the degree of Master of Science in  
Electrical Engineering

Charlotte

2021

Approved by:

---

Dr. Ahmed Arafa

---

Dr. Thomas Weldon

---

Dr. Yawo Amengonu

©2021  
Christopher Daniel Jr.  
ALL RIGHTS RESERVED

## Abstract

CHRISTOPHER DANIEL JR. Timely updating with intermittent energy and data for multiple sources over erasure channels. (Under the direction of DR. AHMED ARAFA)

A status updating system is considered in which multiple data sources generate packets to be delivered to a destination through a *shared* energy harvesting sensor. Only one source's data, when available, can be transmitted by the sensor at a time, subject to energy availability. Transmissions are prone to erasures, and each successful transmission constitutes a status update for its corresponding source at the destination. The goal is to schedule source transmissions such that the *collective* long-term average *age-of-information* (AoI) is minimized. AoI is defined as the time elapsed since the latest successfully-received data has been generated at its source. To solve this problem, the case with a single source is first considered, with a focus on *threshold* waiting policies, in which the sensor attempts transmission only if the time until *both* energy and data are available grows above a certain threshold. The *distribution* of the AoI is fully characterized under such a policy. This is then used to analyze the performance of the multiple sources case under *maximum-age-first* scheduling, in which the sensor's resources are dedicated to the source with the maximum AoI at any given time. The achievable collective long-term average AoI is derived in closed-form. Multiple numerical evaluations are then demonstrated to show how the optimal threshold value behaves as a function of the system parameters, in which showcases the benefits of a threshold-based waiting policy with intermittent energy and data arrivals.

DEDICATION

To my mother, in loving memory.

## ACKNOWLEDGEMENTS

I would like to acknowledge my committee members, each of whom has provided informative advice and guidance throughout the research process. Thank you for your unwavering support of me.

## Contents

LIST OF FIGURES	vii
LIST OF ABBREVIATIONS	viii
PREFACE	1
CHAPTER 1: INTRODUCTION	2
1.1. Related Works	3
CHAPTER 2: SYSTEM MODEL	6
CHAPTER 3: THE SINGLE SOURCE CASE	9
CHAPTER 4: THE MULTIPLE SOURCES CASE	16
CHAPTER 5: NUMERICAL EVALUATIONS	20
CHAPTER 6: CONCLUSION	24
CHAPTER 7: FUTURE WORK	25
Bibliography	26

## List of Figures

FIGURE 1.1: System model overview: status updating with multiple sources using a shared energy harvesting sensor.	3
FIGURE 2.1: An example evolution of the $j$ th source AoI in the $i$ th epoch. Falling (resp. rising) hashed lines rectangles denote failed (resp. successful) attempts for source $j$ , while the solid rectangle denotes other sources' attempts.	8
FIGURE 3.1: An example for the $i$ th epoch evolution with $M_i = 2$ . Circles (resp. squares) represent energy (resp. data) arrivals; a Cross (resp. check mark) represents a failure (resp. success).	10
FIGURE 3.2: An example of a simulated system's empirical CDF of an epoch's starting AoI $\Delta$ under a $\gamma$ -threshold policy vs. the theoretical CDF in (3.11) with $\lambda_e = 1$ , $\lambda_d = 10$ , and $\gamma = 0.9$ .	14
FIGURE 5.1: Optimal threshold $\gamma^*$ versus the erasure probability $q$ , with $\lambda_e = 0.1$ and varying values of $\lambda_d$ .	21
FIGURE 5.2: Percentage gain due to waiting versus the erasure probability, with $\lambda_e = 0.1$ and varying values of $\lambda_d$ .	22
FIGURE 5.3: Optimal threshold $\gamma^*$ versus the number of sources $N$ , with $\lambda_e = 0.1$ , $\lambda_{d,j} = 10$ , $\forall j$ , and varying values of $q$ .	23

## LIST OF ABBREVIATIONS

AoI age-of-information.

CDF cumulative distribution function.

i.i.d. independent and identically distributed.

MAF maximum-age-first.



## Preface

This thesis presents my work on the topic of how to optimize timely updating systems that use the age-of-information metric to effectively quantify the freshness of data transmitted, using an energy harvesting sensor, shared with multiple data sources, through an erasure channel.

## CHAPTER 1: INTRODUCTION

Emerging technological innovations rely on *timely* wireless communications that need to process time critical tasks with up to date information. Low-latency cyber-physical systems which integrate computation, control, and networking have increasing demands for *fresh* information to conduct reliable and efficient tasks. The *age-of-information* (AoI) metric was first introduced in [1] as a novel way to quantify the freshness of knowledge a system has about a process to capture the requirement of such applications as a means to maintain information about the current state of a network, and has since seen growing interests in the literature in various settings demonstrated in the most recent survey [2].

In this thesis, status updating for multiple data sources using a shared energy harvesting sensor over an erasure channel is analyzed. The sources' data and the sensor's energy arrive according to Poisson processes of various rates. The sensor can only serve one data source at a time, with scheduling and transmission policies needed to be designed to optimally manage the arriving energy to transmit the arriving data. The goal is to minimize the *collective* long-term average AoI of all sources at the destination. AoI is defined as the time elapsed since the latest successfully-received data has been generated at its source. We analyze the benefits of idle waiting *after* both energy and data are available for dispatch from a given source, with a focus on *threshold* policies, in which a new transmission occurs only if the time until energy and data arrives surpasses a certain threshold. Idle waiting before updating has been analyzed previously in [3] for a single source, yet in a non-energy-harvesting setting, and with fixed waiting times. In this work, we provide *closed-form* expressions for: (1) the AoI *distribution*; (2) the long-term average AoI for a single source; and (3)

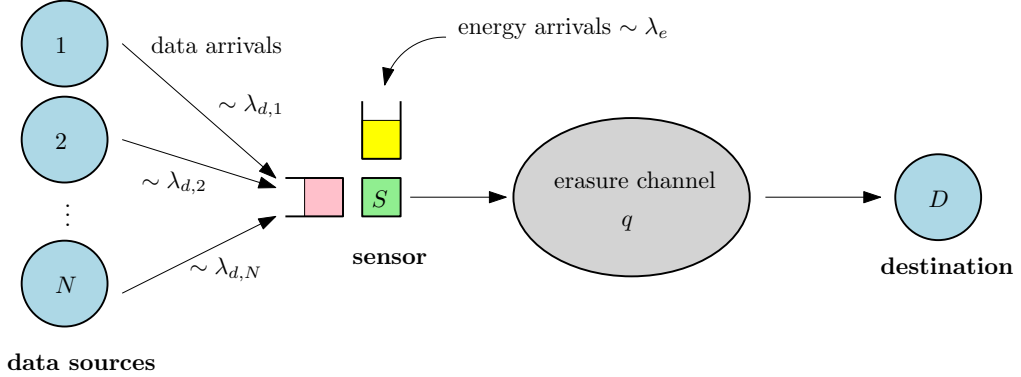


Figure 1.1: System model overview: status updating with multiple sources using a shared energy harvesting sensor.

the collective long-term average AoI for multiple sources under *maximum-age-first* scheduling, in which the source with the maximum AoI is given priority over others. We then show how the optimal threshold value behaves as a function of the system parameters, considering data and energy arrival rates, erasure probability, and the number of data sources attached to the system.

### 1.1 Related Works

Status updating with energy harvesting sensors has been studied in, e.g., [4–24], and can be generally categorized according to whether the energy harvested is known a priori (offline) or causally (online), or whether data can be generated at will or is exogenous. Our work in this thesis is *online with exogenous data arrivals*.

In [4], each status update requires an energy unit and is powered by a stochastic energy harvesting system with an infinite battery. It is demonstrated that waiting is beneficial to reducing the expected AoI in this setting which is an inspiration to our system’s transmission policy. In [5], an energy harvesting sensor continuously monitors the system and sends time-stamped status updates generated at will to a destination which keeps track of the system status through the updates. Optimal online status updating are utilized to minimize the long-term average AoI of a single data source subject to an energy causality constraint for the sensor. Varying battery

sizes of one unit only, finite, and infinite for the system model are also considered.

In [6], an energy harvesting sensor is considered with a random battery recharge model and an incremental battery recharge model. In both models, energy arrives according to a Poisson process which completely fills up the battery in the random battery recharge model, and partially fills up the battery incrementally in the incremental battery recharge model. The optimal status update policy is then examined for both models while showing the optimality of renewal policies, in which the inter-update times follow a renewal process which depends on the energy arrival rate and the size of the battery. The optimal renewal policy is then shown to have a threshold structure, in which a new update is transmitted only if the AoI grows above a certain threshold. Reference [7] shows a similar result to the incremental battery recharge model of [6] for non-decreasing age-penalty functions.

While the works in [5–7] consider generate-at-will models, the works in [8–10] consider exogenous data arrivals, modeled through Poisson processes, as in our setting. Tools from stochastic hybrid systems are employed to analyze the AoI in [8, 9] in different settings, and non-linear age-penalties are considered in [10]. Differently, however, we introduce the notion of threshold waiting before updating and show that it can enhance the achievable AoI under favorable circumstances.

The setting in which updates are subject to being erased is considered in [11] with a finite battery, and in [12, 13] with a unit battery, yet all with generate-at-will sampling system models. In this thesis, we further extend [13] to a model with exogenous data arrivals for multiple data sources.

References [14–16] study multiple data sources. The work in [14] focuses on analyzing the performances of time division multiple access and frequency division multiple access scheduling. Reference [15] follows a Markov decision process framework in a discrete-time setting with a finite time horizon; the optimal policy is such that the sensor first probes the channel if the maximum AoI grows above a certain threshold,

and then decides on sampling the source with the maximum AoI if the probed channel conditions are better than a certain threshold as well. Different from [15], we consider an infinite time horizon setting, with exogenous data arrivals, and provide analytical expressions for the AoI under Poisson energy arrivals. Lastly, the work in [16] considers the notion of source diversity when multiple sources monitor the same physical phenomenon with different costs.

Other related works include focusing on sending information through the timing of status updates [17]; wireless power transfer and RF energy applications [18–21]; heterogeneous data streams [22]; sensing costs [23]; and status priorities [24].

## CHAPTER 2: SYSTEM MODEL

We consider a system composed of  $N$  sources of time-varying data that are to be monitored at a remote destination through the help of a *shared* energy harvesting sensor (transmitter). Source  $j$ 's data is generated in packets according to a Poisson process of rate  $\lambda_{d,j}$ , with each packet containing a time-stamp of its generation time. Each generated data packet is fed into the sensor's data buffer. However, the sensor is capable of only holding *one* data packet at a time, and it needs to decide on whether to discard newly-arriving data packets or preempt the currently-held ones, if any are available for transmission.

Furthermore, the sensor relies on energy harvested from nature to communicate. Energy arrives in units according to a Poisson process of rate  $\lambda_e$ , with each unit capable of transmitting only one data packet. The sensor is equipped with a battery of unit size to save the incoming energy. All processes (sources' data and sensor's energy) are independent. Only when both energy and data are available the sensor may transmit. Transmissions are instantaneous, but are subject to *erasures*; each transmission may get erased with probability  $q$ . Erasure events are i.i.d. across transmissions. The destination also provides instantaneous feedback to denote successful/failed transmissions. An overview of the system model is shown in Fig. 1.1.

Let  $l_{i,j}$  denote the  $i$ th transmission time pertaining to source  $j$ , and  $s_{i,j}$  denote the  $i$ th *successful* transmission of which. Clearly, due to erasures,  $\{s_{i,j}\} \subseteq \{l_{i,j}\}$ . Let us define  $\mathcal{E}(t)$  and  $\mathcal{D}(t)$  as the energy available in the sensor's battery and the identity of the data packet available in the sensor's data buffer at time  $t$ , respectively. Note that  $\mathcal{E}(t) \in \{0, 1\}$ , while  $\mathcal{D}(t) \in \{0, 1, 2, \dots, N\}$ , with  $\mathcal{D}(t) = 0$  denoting an empty data buffer. Therefore, we have the following *energy causality* and *data causality*

constraints [25]:

$$\mathcal{E}(l_{i,j}^-) = 1, \quad \forall i, j, \quad (2.1)$$

$$\mathcal{D}(l_{i,j}^-) = j, \quad \forall i, j, \quad (2.2)$$

where  $l_{i,j}^-$  denotes the time instant right before  $l_{i,j}$ . A set of feasible  $\{l_{i,j}\}$  according to (2.1) and (2.2) is denoted the *transmission policy*. We denote this by  $\pi$ , a *scheduling policy* that determines how the sensor manages its data buffer, e.g., which data source is to be given priority. Observe that the transmission policy is, in general, highly intertwined with the scheduling policy.

Our main metric of focus is data freshness, captured effectively through AoI. When a transmission for source  $j$ 's data is successful, a *status update* is received at the destination. Thus, the AoI for source  $j$  at time  $t$  is defined as

$$a_j(t) \triangleq t - u_j(t), \quad (2.3)$$

where  $u_j(t)$  is the time-stamp of the latest successfully-received data pertaining to source  $j$ . An example of how the AoI may evolve over time is shown in Fig. 2.1. We use the term *epoch* to denote the time in between two consecutive successful transmissions for a given source. For source  $j$ 's  $i$ th epoch, we denote its starting AoI by  $\Delta_{i-1,j}$ , its length by  $L_{i,j}$ , and the corresponding area under the AoI evolution curve during which by  $Q_{i,j}$ , see Fig. 2.1. From the figure, one can see that

$$L_{i,j} = s_{i,j} - s_{i-1,j}, \quad (2.4)$$

$$Q_{i,j} = \Delta_{i-1,j} L_{i,j} + \frac{1}{2} L_{i,j}^2. \quad (2.5)$$

The goal is to design transmission and scheduling policies to minimize the *collective* long-term average AoI of all data sources. That is, to solve the following optimization

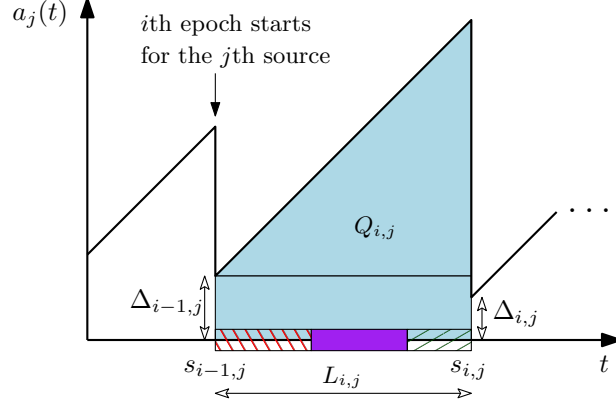


Figure 2.1: An example evolution of the  $j$ th source AoI in the  $i$ th epoch. Falling (resp. rising) hashed lines rectangles denote failed (resp. successful) attempts for source  $j$ , while the solid rectangle denotes other sources' attempts.

problem:

$$\begin{aligned}
 \min_{\{l_{i,j}\}, \pi} \quad & \frac{1}{N} \sum_{j=1}^N \limsup_{n \rightarrow \infty} \frac{\sum_{i=1}^n \mathbb{E}[Q_{i,j}]}{\sum_{i=1}^n \mathbb{E}[L_{i,j}]} \\
 \text{s.t.} \quad & \mathcal{E}(l_{i,j}^-) = 1, \quad \forall i, j, \\
 & \mathcal{D}(l_{i,j}^-) = j, \quad \forall i, j,
 \end{aligned} \tag{2.6}$$

where the expectation  $\mathbb{E}[\cdot]$  is taken according to the underlying energy, data, and erasure distributions.

We discuss the solution of problem (2.6) over the next two chapters, first for the single source case, followed by the multiple sources case.



### CHAPTER 3: THE SINGLE SOURCE CASE

In this chapter, we focus on problem (2.6) for  $N = 1$  data source, which will serve as a necessary building block for  $N \geq 2$ . In this case, no scheduling is needed, and hence we drop the index  $j$ . Since we aim at minimizing AoI, only the freshest data packet is kept at the sensor's data buffer, i.e., newly-generated data packets preempt old ones waiting for transmission, if any are available.

Let  $e_{i,1}$  and  $d_{i,1}$  denote the time elapsed from the beginning of the  $i$ th epoch until the first energy and data arrivals, respectively. It then follows that  $e_{i,1} \sim \exp(\lambda_e)$  and  $d_{i,1} \sim \exp(\lambda_d)$ . By (2.1) and (2.2), the first transmission attempt in the  $i$ th epoch must therefore occur after at least  $\max\{e_{i,1}, d_{i,1}\}$  time units. Instead of transmitting right when energy and data are available, we allow the sensor to idly *wait* for some extra time units. While this lets the current data packet become more stale, *it provides an opportunity for the sensor to capture a fresher data packet in the waiting window before transmission*. Specifically, the first transmission attempt in the  $i$ th epoch occurs after

$$w(\max\{e_{i,1}, d_{i,1}\}) \tag{3.1}$$

time units from its beginning, for some waiting function  $w(t) \geq t$ . If such a transmission attempt fails, the above policy is repeated, yet with  $e_{i,2}$  and  $d_{i,2}$ , which now denote the time until the next energy and data arrivals, respectively, *after* the first transmission attempt. By the memoryless property of the exponential distribution,  $e_{i,2} \sim \exp(\lambda_e)$  and  $d_{i,2} \sim \exp(\lambda_d)$  as well. Transmission attempts are required to continue until success. Let  $M_i$  denote the number of transmission attempts during

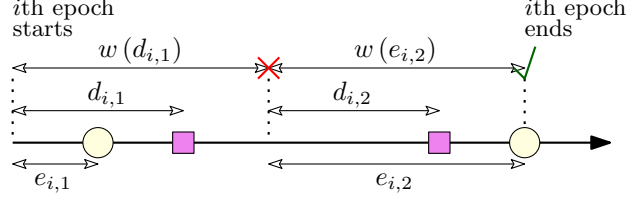


Figure 3.1: An example for the  $i$ th epoch evolution with  $M_i = 2$ . Circles (resp. squares) represent energy (resp. data) arrivals; a Cross (resp. check mark) represents a failure (resp. success).

the  $i$ th epoch. It is direct to see that  $M_i$ 's are i.i.d. geometrically-distributed with parameter  $1 - q$ . Therefore, one can write

$$L_i = \sum_{k=1}^{M_i} w(\max\{e_{i,k}, d_{i,k}\}). \quad (3.2)$$

An example is shown in Fig. 3.1.

Next, observe that the proposed transmission/waiting policy induces a *stationary* distribution across all epochs. Since  $w(\max\{e_{i,k}, d_{i,k}\})$ 's are i.i.d., and since  $M_i$  is independent of  $w(\max\{e_{i,k}, d_{i,k}\})$ , one can use Wald's identity to write

$$\begin{aligned} \mathbb{E}[L_i] &= \mathbb{E}[M_i] \mathbb{E}[w(\max\{e_i, d_i\})] \\ &= \frac{\mathbb{E}[w(\max\{e_i, d_i\})]}{1 - q}, \quad \forall i, \end{aligned} \quad (3.3)$$

$$\begin{aligned} \mathbb{E}[L_i^2] &= \mathbb{E}[M_i] \mathbb{E}[w(\max\{e_i, d_i\})^2] + \mathbb{E}[M_i(M_i - 1)] (\mathbb{E}[w(\max\{e_i, d_i\})])^2 \\ &= \frac{\mathbb{E}[w(\max\{e_i, d_i\})^2]}{1 - q} + \frac{2q (\mathbb{E}[w(\max\{e_i, d_i\})])^2}{(1 - q)^2}, \quad \forall i, \end{aligned} \quad (3.4)$$

where the second equalities in (3.3) and (3.4) follow from the properties of the geometric distribution. In addition, we note that  $\Delta_{i-1}$  is now independent of  $L_i$ . Hence,

$$\mathbb{E}[Q_i] = \mathbb{E}[\Delta_{i-1}] \mathbb{E}[L_i] + \frac{1}{2} \mathbb{E}[L_i^2], \quad \forall i. \quad (3.5)$$

Using (3.3), (3.4), and (3.5), problem (2.6) now reduces to the following optimization

problem over a typical epoch:

$$\min_{w(t) \geq t} \mathbb{E}[\Delta_{i-1}] + \frac{\mathbb{E}[L_i^2]}{2\mathbb{E}[L_i]}. \quad (3.6)$$

For a given waiting policy  $w(\cdot)$ , the following lemma characterizes the CDF of the starting AoI  $\Delta_{i-1}$ . By stationarity, we drop the index  $i$  for simplicity of the presentation in the remainder of this chapter.

**Lemma 1** *The CDF of an epoch's starting AoI  $\Delta$  is given by*

$$F_{\Delta}(\delta) = 1 - e^{-\lambda_d \delta} P(w(\max\{e, d\}) - d \geq \delta), \quad \delta \geq 0. \quad (3.7)$$

**Proof:** We first note that  $\Delta$  only depends on the variables pertaining to the successful (final) transmission attempt in the epoch, and does not depend on how many failures  $M - 1$  occurred before it. Thus, the random variables  $e$  and  $d$  denote the time until the energy and data arrivals, respectively, since the  $(M - 1)$ th transmission attempt.

We now use total probability to write

$$F_{\Delta}(\delta) = \int_{t_e, t_d \geq 0} P(\Delta \leq \delta | e = t_e, d = t_d) f_{e,d}(t_e, t_d) dt_e dt_d, \quad (3.8)$$

with  $f_{e,d}(t_e, t_d) \triangleq \lambda_e e^{-\lambda_e t_e} \lambda_d e^{-\lambda_d t_d}$ . Now observe that if  $w(\max\{t_e, t_d\}) - t_d < \delta$ , then clearly  $P(\Delta \leq \delta | e = t_e, d = t_d) = 1$ . On the other hand, if  $w(\max\{t_e, t_d\}) - t_d \geq \delta$ , then  $\Delta \leq \delta$  if and only if at least one data arrival occurred in the *last  $\delta$  interval of the epoch*. The memoryless property of the exponential distribution indicates that  $P(\Delta \leq \delta | e = t_e, d = t_d) = 1 - e^{-\lambda_d \delta}$  in this case. Combining both cases we get

$$F_{\Delta}(\delta) = 1 - e^{-\lambda_d \delta} \int_{t_e, t_d: w(\max\{t_e, t_d\}) - t_d \geq \delta} f_{e,d}(t_e, t_d) dt_e dt_d, \quad (3.9)$$

which is exactly (3.7). ■

We observe that solving problem (3.6) is challenging since the waiting function is embedded into the CDF of  $\Delta$  in a highly intertwined manner as shown in (3.7). Inspired by the results in [5–7,12,13] we focus on *threshold* waiting policies and analyze their performance. These threshold waiting policies are defined as

$$w(t) = t + [\gamma - t]^+, \quad (3.10)$$

for some  $\gamma \geq 0$ , where  $[\cdot]^+ \triangleq \max(\cdot, 0)$ . Thus, a new transmission attempt takes effect only if the time until its pertaining energy and data become available surpasses a certain threshold  $\gamma$ . Threshold policies are quite intuitive, since one needs to balance the risk of waiting too long and letting the available data grow stale, with that of waiting too short and missing the opportunity to capture fresher available data. In addition, they have been shown optimal in, e.g., [5–7, 12, 13], albeit in a generate-at-will context in which data arrivals times are controlled. Under the specific  $\gamma$ -threshold policies introduced in (3.10), the next lemma characterizes the distribution of the starting AoI of each epoch.

**Lemma 2** *Under a  $\gamma$ -threshold policy, the CDF of an epoch's starting AoI  $\Delta$  is given by*

$$F_{\Delta}(\delta) = 1 - e^{-\lambda_d \delta} \left( 1 - e^{-\lambda_d [\gamma - \delta]^+} \left( 1 - \frac{\lambda_d}{\lambda_e + \lambda_d} e^{-\lambda_e \max\{\gamma, \delta\}} \right) \right), \quad \delta \geq 0. \quad (3.11)$$

**Proof:** We show this by substituting (3.10) into (3.7) and evaluating the inner probability terms. Taking this route, we have

$$\begin{aligned} P(d \geq e, [\gamma - d]^+ \geq \delta) &= \int_{t_d=0}^{[\gamma - \delta]^+} \int_{t_e=0}^{t_d} f_{e,d}(t_e, t_d) dt_e dt_d \\ &= 1 - e^{-\lambda_d [\gamma - \delta]^+} - \frac{\lambda_d}{\lambda_d + \lambda_e} \left( 1 - e^{-(\lambda_e + \lambda_d) [\gamma - \delta]^+} \right). \end{aligned} \quad (3.12)$$

We deal with the other probability term by dividing it into two integrals in which  $e > \gamma$  and  $e \leq \gamma$  as follows:

$$P(d \leq e, [\gamma - e]^+ + e - d \geq \delta) = \int_{t_e = \max\{\gamma, \delta\}}^{\infty} \int_{t_d = 0}^{t_e - \delta} f_{e,d}(t_e, t_d) dt_d dt_e \\ + \int_{t_e = 0}^{\gamma} \int_{t_d = 0}^{\min\{t_e, [\gamma - \delta]^+\}} f_{e,d}(t_e, t_d) dt_d dt_e. \quad (3.13)$$

One can show that the first integral is equal to

$$e^{-\lambda_e \max\{\gamma, \delta\}} - \frac{\lambda_e}{\lambda_e + \lambda_d} e^{-(\lambda_e + \lambda_d) \max\{\gamma, \delta\}} e^{\lambda_d \delta}, \quad (3.14)$$

and that the second one is equal to

$$1 - e^{-\lambda_e [\gamma - \delta]^+} - \frac{\lambda_e}{\lambda_d + \lambda_e} \left(1 - e^{-(\lambda_e + \lambda_d) [\gamma - \delta]^+}\right) + \left(1 - e^{-\lambda_d [\gamma - \delta]^+}\right) \left(e^{-\lambda_e [\gamma - \delta]^+} - e^{-\lambda_e \gamma}\right). \quad (3.15)$$

Adding (3.12), (3.14), and (3.15) together with some involved algebraic manipulations, one can achieve the simplified expression of (3.11). ■

In Fig. 3.2, we show an example of a simulated system's empirical CDF of an epoch's starting AoI  $\Delta$  under a  $\gamma$ -threshold policy vs. the theoretical CDF in (3.11) with  $\lambda_e = 1$ ,  $\lambda_d = 10$ , and  $\gamma = 0.9$ . We see from the figure that the theoretical and empirical CDFs are practically indistinguishable.

Using the CDF in (3.11), one can now compute the average starting AoI of the epoch as follows:

$$\mathbb{E}[\Delta] = \int_0^{\infty} (1 - F_{\Delta}(\delta)) d\delta \\ = \frac{(1 - e^{-\lambda_d \gamma})}{\lambda_d} - \gamma e^{-\lambda_d \gamma} \left(1 - \frac{\lambda_d}{\lambda_e + \lambda_d} e^{-\lambda_e \gamma}\right) + \frac{\lambda_d}{(\lambda_e + \lambda_d)^2} e^{-(\lambda_e + \lambda_d) \gamma}. \quad (3.16)$$

Next, we evaluate the first and second moments of the epoch length  $L$  in (3.3)

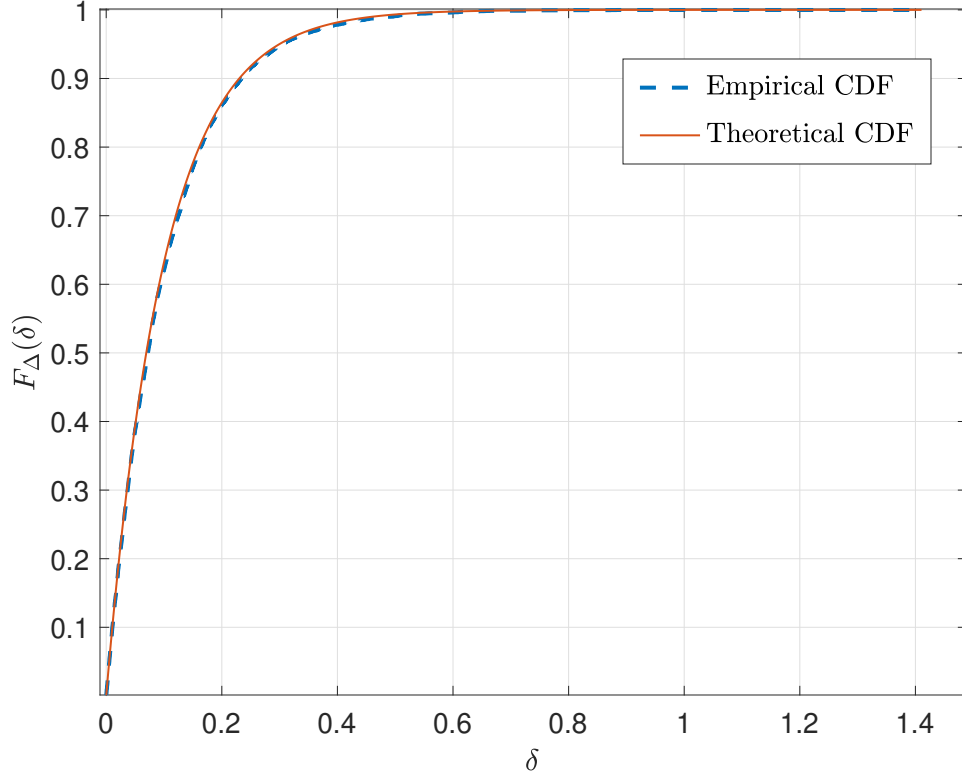


Figure 3.2: An example of a simulated system's empirical CDF of an epoch's starting AoI  $\Delta$  under a  $\gamma$ -threshold policy vs. the theoretical CDF in (3.11) with  $\lambda_e = 1$ ,  $\lambda_d = 10$ , and  $\gamma = 0.9$ .

and (3.4), respectively, by evaluating the first and second moments of  $w(\max\{e, d\})$ .

Direct computations lead to the following result for the first moment:

$$\begin{aligned}
& \mathbb{E}[w(\max\{e, d\})] \\
&= \gamma(1 - e^{-\lambda_d\gamma})(1 - e^{-\lambda_e\gamma}) + \frac{(\lambda_d\gamma + 1)}{\lambda_d} e^{-\lambda_d\gamma}(1 - e^{-\lambda_e\gamma}) + \frac{(\lambda_e\gamma + 1)}{\lambda_e} e^{-\lambda_e\gamma}(1 - e^{-\lambda_d\gamma}) \\
&+ \frac{\lambda_d[\lambda_e(\lambda_e + \lambda_d)\gamma + 2\lambda_e + \lambda_d]}{\lambda_e(\lambda_e + \lambda_d)^2} e^{-(\lambda_e + \lambda_d)\gamma} + \frac{\lambda_e[\lambda_d(\lambda_e + \lambda_d)\gamma + 2\lambda_d + \lambda_e]}{\lambda_d(\lambda_e + \lambda_d)^2} e^{-(\lambda_e + \lambda_d)\gamma}.
\end{aligned} \tag{3.17}$$

For the second moment, the computations lead to a more involved expression,

$$\begin{aligned}
& \mathbb{E} [w (\max\{e, d\})^2] \\
&= \gamma^2 (1 - e^{-\lambda_d \gamma}) (1 - e^{-\lambda_e \gamma}) + \frac{\lambda_d^2 \gamma^2 + 2\lambda_d \gamma + 2}{\lambda_d^2} e^{-\lambda_d \gamma} (1 - e^{-\lambda_e \gamma}) \\
&+ \frac{\lambda_e^2 \gamma^2 + 2\lambda_e \gamma + 2}{\lambda_e^2} e^{-\lambda_e \gamma} (1 - e^{-\lambda_d \gamma}) \\
&+ \frac{\lambda_d (\lambda_e^2 (\lambda_e + \lambda_d)^2 \gamma^2 + 2\lambda_e (\lambda_e + \lambda_d) (2\lambda_e + \lambda_d) \gamma + 6\lambda_e^2 + 6\lambda_e \lambda_d + 2\lambda_d^2)}{\lambda_e^2 (\lambda_e + \lambda_d)^3} e^{-(\lambda_e + \lambda_d) \gamma} \\
&+ \frac{\lambda_e (\lambda_d^2 (\lambda_e + \lambda_d)^2 \gamma^2 + 2\lambda_d (\lambda_e + \lambda_d) (2\lambda_d + \lambda_e) \gamma + 6\lambda_d^2 + 6\lambda_e \lambda_d + 2\lambda_e^2)}{\lambda_d^2 (\lambda_e + \lambda_d)^3} e^{-(\lambda_e + \lambda_d) \gamma}.
\end{aligned} \tag{3.18}$$

Finally, using (3.16), (3.17), and (3.18), together with (3.3) and (3.4), one can substitute these expressions into (3.6) and evaluate the long-term average AoI achieved with a  $\gamma$ -threshold policy. We define this as  $\overline{\text{AoI}}_q(\gamma)$  to appropriately emphasize the dependency on  $q$  and  $\gamma$ .

## CHAPTER 4: THE MULTIPLE SOURCES CASE

In this chapter, we extend the results of chapter 3 to  $N \geq 2$  sources. We consider a MAF scheduling policy, denoted  $\pi_{MAF}$ , in which the sensor's data buffer accepts data packets from source  $j$  at time  $t$  if and only if it has the maximum instantaneous AoI, i.e., if and only if  $a_j(t) \geq a_\kappa(t)$ ,  $\forall \kappa \neq j$ . Let us assume without loss of generality that the system starts with fresh information at time 0:  $a_j(0) = 0$ ,  $\forall j$ , and hence, under the  $\pi_{MAF}$  scheduling policy, the sensor first dedicates all transmission attempts to source 1's data, until successful, and then focuses on source 2's data, all the way until source  $N$ 's data is transmitted successfully, and then repeats transmission attempts in the same order  $\{1, 2, \dots, N\}$ . We also note that MAF scheduling is only possible due to the erasure status feedback made available by the destination.

Let us focus on some source  $j$ , and denote by  $e_{i,1}^{(j)}$  and  $d_{i,1}^{(j)}$  the time elapsed from the beginning of the  $i$ th epoch until the first energy and data arrivals, respectively, dedicated for that source. As in Chapter 3, the sensor does not immediately attempt transmission after receiving the energy and data. Instead, the first transmission attempt for source  $j$  in the  $i$ th epoch occurs after

$$w \left( \max \left\{ e_{i,1}^{(j)}, d_{i,1}^{(j)} \right\} \right) \tag{4.1}$$

time units from its beginning. This is followed by a second attempt in case of failure, which occurs after another  $w \left( \max \left\{ e_{i,2}^{(j)}, d_{i,2}^{(j)} \right\} \right)$  time units, where  $e_{i,2}^{(j)}$  and  $d_{i,2}^{(j)}$  now denote the time until the next energy and data arrivals, respectively, for source  $j$  *after* the first transmission attempt. This continues until source  $j$ 's transmission is successful, which takes  $M_{j,i}$  attempts. Afterwards, the focus turns to source  $j + 1$ .



Observe that  $M_{j,i}$ 's are i.i.d. geometric random variables with parameter  $1 - q$ . In addition, by the memoryless property of exponential distribution,  $e_{i,k}^{(j)} \sim \exp(\lambda_e)$  and  $d_{i,k}^{(j)} \sim \exp(\lambda_{d,j})$ ,  $\forall i, k$ . The structure of our waiting policy, therefore, induces a stationary distribution across all epochs. Therefore, we drop the index  $i$ , and define the following random variables in a typical epoch for source  $j$ :  $\Delta^{(j)}$  as the starting AoI;  $L^{(j)}$  as the epoch length; and  $Q^{(j)}$  as the area under the AoI evolution curve in the epoch. Therefore, one can write

$$\mathbb{E}[Q^{(j)}] = \mathbb{E}[\Delta^{(j)}] \mathbb{E}[L^{(j)}] + \frac{1}{2} \mathbb{E}[(L^{(j)})^2]. \quad (4.2)$$

As in chapter 3, we focus on  $\gamma$ -threshold waiting policies in our analysis. We use the same threshold  $\gamma$  for all sources. The analysis is readily extendable to account for different thresholds if needed. Now observe that under  $\pi_{MAF}$ , source  $j$ 's epoch length depends on the time elapsed until *all other sources are done with their successful transmissions*. With a slight abuse of notation, let us denote by  $L_\kappa$  the time needed for source  $\kappa$  to finish its successful transmission. Therefore, one can express

$$L^{(j)} = \sum_{\kappa=1}^N L_\kappa \quad (4.3)$$

in a typical epoch. We now present the main result.

**Theorem 1** *Let  $\overline{AoI}_{q,N}(MAF, \gamma)$  denote the collective long-term average AoI of prob-*

lem (2.6) achieved under  $\pi_{MAF}$  and  $\gamma$ -threshold waiting policy. Then

$$\begin{aligned} \overline{AoI}_{q,N}(MAF, \gamma) &= \frac{1}{N} \sum_{j=1}^N \mathbb{E} [\Delta^{(j)}] + \frac{\sum_{\kappa=1}^N \mathbb{E} [w(\max\{e^{(\kappa)}, d^{(\kappa)}\})^2]}{2 \sum_{\kappa=1}^N \mathbb{E} [w(\max\{e^{(\kappa)}, d^{(\kappa)}\})]} \\ &\quad + \frac{q \sum_{\kappa=1}^N (\mathbb{E} [w(\max\{e^{(\kappa)}, d^{(\kappa)}\})])^2}{(1-q) \sum_{\kappa=1}^N \mathbb{E} [w(\max\{e^{(\kappa)}, d^{(\kappa)}\})]} \\ &\quad + \frac{\sum_{\substack{1 \leq \alpha \leq N \\ 1 \leq \beta < \alpha}} \mathbb{E} [w(\max\{e^{(\alpha)}, d^{(\alpha)}\})] \mathbb{E} [w(\max\{e^{(\beta)}, d^{(\beta)}\})]}{(1-q) \sum_{\kappa=1}^N \mathbb{E} [w(\max\{e^{(\kappa)}, d^{(\kappa)}\})]}, \end{aligned} \quad (4.4)$$

with  $\mathbb{E} [\Delta^{(j)}]$  given by (3.16) after replacing  $\lambda_d$  with  $\lambda_{d,j}$ , and the first and second moments of  $w(\max\{e^{(\kappa)}, d^{(\kappa)}\})$  given by (3.17) and (3.18), respectively, after replacing  $\lambda_d$  with  $\lambda_{d,\kappa}$ .

**Proof:** It is clear from (4.3) that  $L^{(j)}$ 's are i.i.d. across sources  $\sim L^{(*)}$ . By (4.2), one can express  $\overline{AoI}_{q,N}(MAF, \gamma)$  as

$$\frac{1}{N} \sum_{j=1}^N \mathbb{E} [\Delta^{(j)}] + \frac{\mathbb{E} [(L^{(*)})^2]}{2\mathbb{E} [L^{(*)}]}. \quad (4.5)$$

Now observe that the average starting AoI  $\mathbb{E} [\Delta^{(j)}]$  will be given by (3.16) after replacing  $\lambda_d$  by  $\lambda_{d,j}$ , since the same  $\gamma$ -threshold policy is applied at every transmission attempt. Thus, it only remains to evaluate the first and second moments of  $L^{(*)}$ . Towards that end, using (4.3), one can write

$$\mathbb{E} [L^{(*)}] = \sum_{\kappa=1}^N \mathbb{E} [L_{\kappa}], \quad (4.6)$$

$$\mathbb{E} [(L^{(*)})^2] = \sum_{\kappa=1}^N \mathbb{E} [(L_{\kappa})^2] + 2 \sum_{\alpha=1}^N \sum_{\beta=1}^{\alpha-1} \mathbb{E} [L_{\alpha}] \mathbb{E} [L_{\beta}]. \quad (4.7)$$

Next, we note that the first and second moments of  $L_{\kappa}$  are given by (3.3) and (3.4), respectively, in which the corresponding first and second moments of the waiting random variables are given by (3.17) and (3.18), respectively, after replacing  $\lambda_d$  with

$\lambda_{d,\kappa}$ . Substituting these results into (4.5) and then simplifying gives us our main result in (4.4). ■

## CHAPTER 5: NUMERICAL EVALUATIONS

We now present various numerical evaluations to further illustrate the results of this thesis. We first show how the optimal threshold value behaves as a function of the system parameters for the single source case. In all experiments, we set the energy arrival rate to  $\lambda_e = 0.1$ . In Fig. 5.1, we plot the optimal threshold  $\gamma^*$  that minimizes  $\overline{\text{AoI}}_q(\gamma)$  versus the erasure probability  $q$ , with varying values of  $\lambda_d$ . One can see that as the erasure probability increases, the optimal threshold value decreases, which demonstrates that waiting for additional data to arrive is not beneficial for the AoI due to the increased rate of erased data transmissions in our system. We also observe that as the data arrival rate approaches the energy arrival rate, the optimal threshold value decreases. This shows that *waiting is more beneficial to reducing the AoI when  $\lambda_d$  is relatively larger than  $\lambda_e$ , and when  $q$  is relatively small.*

In Fig. 5.2, we plot the *percentage gain due to waiting* versus the erasure probability. We define the percentage gain as

$$\left(1 - \frac{\overline{\text{AoI}}_q(\gamma^*)}{\overline{\text{AoI}}_q(0)}\right) \times 100\%. \quad (5.1)$$

That is, the percentage amount of *reward* one can gain by applying the optimal threshold waiting policy when compared to a *zero-wait* policy. From the figure, it can be seen that as the data arrival rate approaches the energy arrival rate, there is no percentage gain to waiting for additional data arrivals. However, as the data arrival rate becomes relatively larger than the energy arrival rate, waiting becomes significantly beneficial with the corresponding optimal threshold value shown in Fig. 5.1. In addition, since  $\gamma^*$  approaches 0 as  $q$  increases, we see that the percentage gain due to

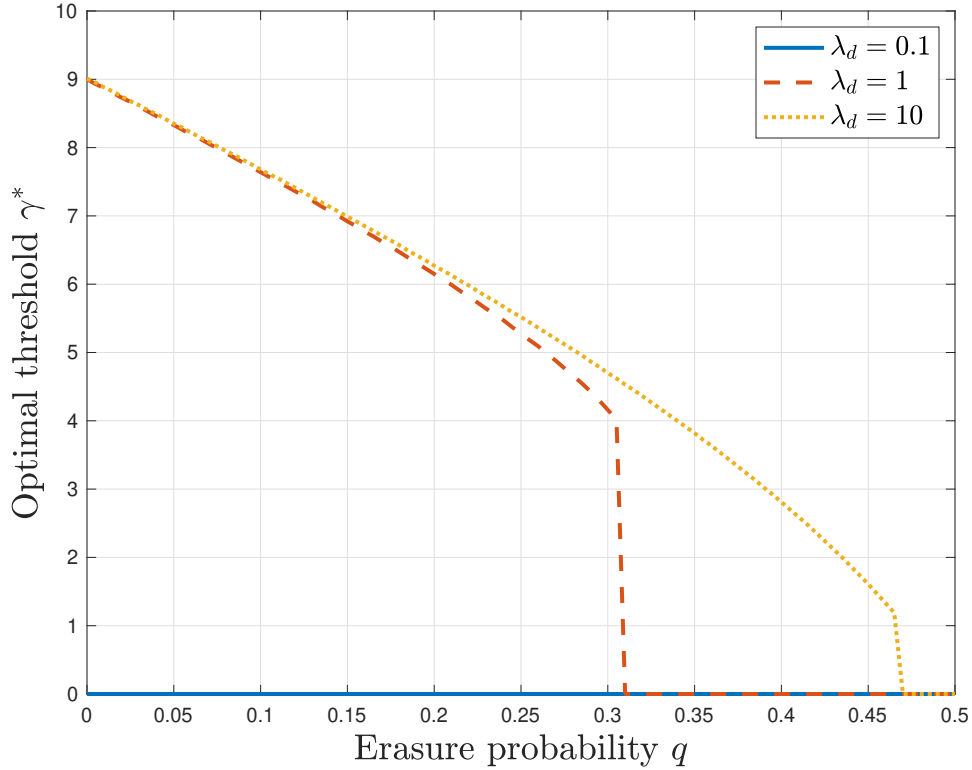


Figure 5.1: Optimal threshold  $\gamma^*$  versus the erasure probability  $q$ , with  $\lambda_e = 0.1$  and varying values of  $\lambda_d$ .

waiting decreases with the increase in erasure probability as well. Finally, though it is not shown on the figure, we observe, numerically, that for  $\lambda_d > 10$ , the percentage gain curve is almost the same as that for  $\lambda_d = 10$ . This may be attributed to the fact that the sensor's battery is unit-sized, and therefore higher gains from waiting could be achieved for larger battery sizes in future work.

Next, we present results for the multiple sources case. For that, we focus on a *symmetric* system in which all data arrivals' rates are the same, i.e.,  $\lambda_{d,j} = \lambda_d, \forall j$ . Hence, we drop the sources' indices from (4.4), since every random variable now is

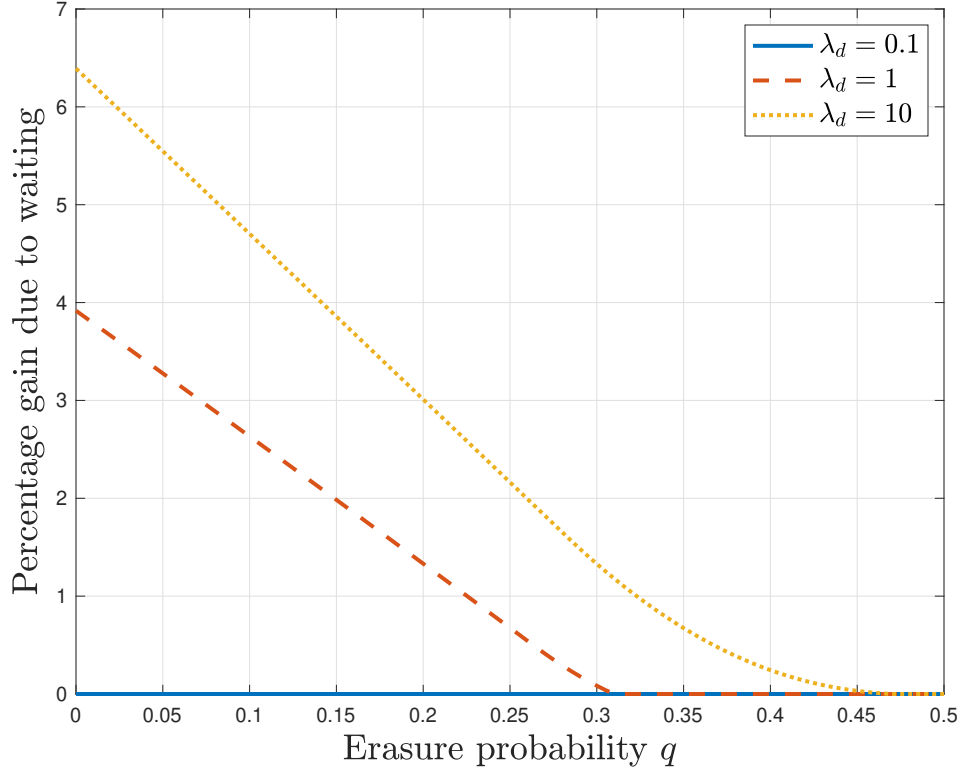


Figure 5.2: Percentage gain due to waiting versus the erasure probability, with  $\lambda_e = 0.1$  and varying values of  $\lambda_d$ .

identical, and simplify the expression to obtain

$$\overline{\text{AoI}}_{q,N}(MAF, \gamma) = \mathbb{E}[\Delta] + \frac{\mathbb{E}[(w(\max\{e, d\}))^2]}{2\mathbb{E}[w(\max\{e, d\})]} + \left( \frac{q + \frac{N-1}{2}}{1-q} \right) \mathbb{E}[w(\max\{e, d\})]. \quad (5.2)$$

It is immediate to see that the collective long-term average AoI is increasing in both the number of sources  $N$  and the erasure probability  $q$ . In Fig. 5.3, we show how the optimal threshold  $\gamma^*$  behaves as a function of  $N$  and  $q$ . Fig. 5.3 demonstrates that as the number of sources grow relatively large, there is no benefit to waiting for additional data arrivals and the corresponding optimal threshold policy becomes a zero-wait policy. This is mainly due to the fact that as the number of sources increase, each source's inter-update duration becomes *longer*, since they need to wait

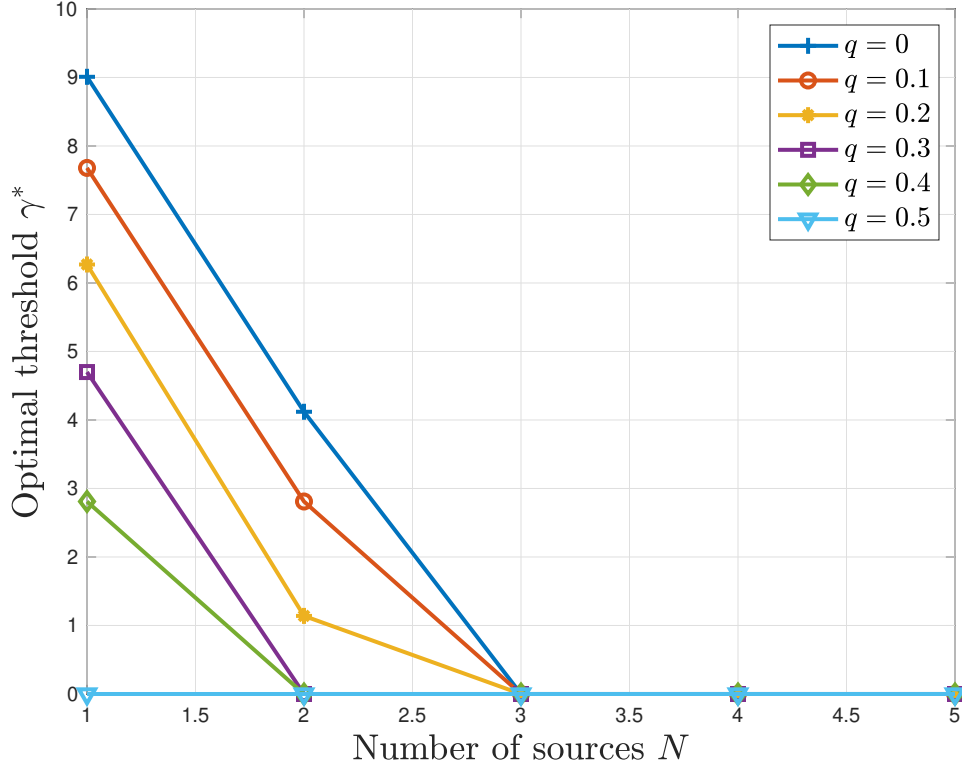


Figure 5.3: Optimal threshold  $\gamma^*$  versus the number of sources  $N$ , with  $\lambda_e = 0.1$ ,  $\lambda_{d,j} = 10$ ,  $\forall j$ , and varying values of  $q$ .

for every other source's successful transmission under the  $\pi_{MAF}$  policy. It is also shown in Fig. 5.3, as in Figs. 5.1 and 5.2, that the optimal threshold value decreases as a function of  $q$ . Once  $q = 0.5$ , the optimal threshold values become 0 for any number of sources, which agrees with the data demonstrated in Figs. 5.1 and 5.2. This also resonates with the results shown in the generate-at-will single source study of [12], in which a zero-waiting policy is optimal if  $q \geq 0.5$ .

## CHAPTER 6: CONCLUSION

A multiple source status updating system has been considered, in which data is generated according to Poisson processes and are conveyed to a destination over an erasure channel using a shared energy harvesting sensor. Detailed analyses of the achievable collective long-term average AoI of the sources have been carried out with a focus on threshold-based transmission policies combined with the maximum-age-first scheduling policy, showcasing the benefits of waiting before updating in such systems and extending previous works in the literature.



## CHAPTER 7: FUTURE WORK

Future work includes analyzing other scheduling policies for sensors with larger data buffers and battery sizes. These additional data buffers and battery sizes could very well contribute to additional percentage gain due to waiting at the expense of a more laborious analysis of the system.

The MAF scheduling policy may be the optimal policy when the data arrivals' rates are the same, i.e., when the system parameters are symmetric across sources. However, when the data arrivals' rates are not the same, and we evaluate a non-symmetric system, different scheduling policies are necessary to enhance the performance of the model and solve problem (2.6) optimally.

Finally, extending the analyses done for arbitrary energy and data arrival processes that are not necessarily Poisson could be pursued, so as to model more general and practical systems. It is expected, however, that closed-form solutions in these cases would not be direct to achieve with intensive numerical work required to utilize these system models.

## Bibliography

- [1] S. Kaul, M. Gruteser, V. Rai, and J. Kenney, “Minimizing age of information in vehicular networks,” in *IEEE SECON*, June 2011.
- [2] R. D. Yates, Y. Sun, D. R. B. III, S. K. Kaul, E. Modiano, and S. Ulukus, “Age of information: An introduction and survey.” Available Online: arXiv:2007.08564.
- [3] P. Zou, O. Ozel, and S. Subramaniam, “Waiting before serving: A companion to packet management in status update systems,” *IEEE Trans. Inf. Theory*, vol. 66, pp. 3864–3877, June 2020.
- [4] R. D. Yates, “Lazy is timely: Status updates by an energy harvesting source,” in *Proc. IEEE ISIT*, June 2015.
- [5] X. Wu, J. Yang, and J. Wu, “Optimal status update for age of information minimization with an energy harvesting source,” *IEEE Trans. Green Commun. Netw.*, vol. 2, pp. 193–204, March 2018.
- [6] A. Arafa, J. Yang, S. Ulukus, and H. V. Poor, “Age-minimal transmission for energy harvesting sensors with finite batteries: Online policies,” *IEEE Trans. Inf. Theory*, vol. 66, pp. 534–556, January 2020.
- [7] B. T. Bacinoglu, Y. Sun, E. Uysal-Biyikoglu, and V. Mutlu, “Optimal status updating with a finite-battery energy harvesting source,” *J. Commun. Netw.*, vol. 21, pp. 280–294, June 2019.
- [8] S. Farazi, A. G. Klein, and D. R. B. III, “Average age of information for status update systems with an energy harvesting server,” in *Proc. IEEE Infocom*, April 2018.
- [9] S. Farazi, A. G. Klein, and D. R. B. III, “Age of information in energy harvesting status update systems: When to preempt in service?,” in *Proc. IEEE ISIT*, June 2018.
- [10] X. Zheng, S. Zhou, Z. Jiang, and Z. Niu, “Closed-form analysis of non-linear age-of-information in status updates with an energy harvesting transmitter,” *IEEE Trans. Wireless Commun.*, vol. 18, pp. 4129–4142, August 2019.
- [11] S. Feng and J. Yang, “Age of information minimization for an energy harvesting source with updating erasures: Without and with feedback.” Available Online: arXiv:1808.05141.
- [12] A. Arafa, J. Yang, S. Ulukus, and H. V. Poor, “Online timely status updates with erasures for energy harvesting sensors,” in *Proc. Allerton*, October 2018.
- [13] A. Arafa, J. Yang, S. Ulukus, and H. V. Poor, “Using erasure feedback for online timely updating with an energy harvesting sensor,” in *Proc. IEEE ISIT*, July 2019.

- [14] N. Hirosawa, H. Iimori, K. Ishibashi, and G. T. F. D. Abreu, “Minimizing age of information in energy harvesting wireless sensor networks,” *IEEE Access*, vol. 8, pp. 219934–219945, 2020.
- [15] A. Jaiswal and A. Chattopadhyay, “Minimization of age-of-information in remote sensing with energy harvesting.” Available Online: arXiv:2010.07626.
- [16] E. Gindullina, L. Badia, and D. Gunduz, “Age-of-information with information source diversity in an energy harvesting system.” Available Online: arXiv:2004.11135.
- [17] A. Baknina, O. Ozel, J. Yang, S. Ulukus, and A. Yener, “Sending information through status updates,” in *Proc. IEEE ISIT*, June 2018.
- [18] I. Krikidis, “Average age of information in wireless powered sensor networks,” *IEEE Wireless Commun. Lett.*, vol. 8, pp. 628–631, April 2019.
- [19] H. Ko, H. Lee, T. Kim, and S. Pack, “Information freshness-guaranteed and energy-efficient data generation control system in energy harvesting internet of things,” *IEEE Access*, vol. 8, pp. 168711–168720, 2020.
- [20] M. A. Abd-Elmagid, H. S. Dhillon, and N. Pappas, “AoI-optimal joint sampling and updating for wireless powered communication systems.” Available Online: arXiv:2006.06339.
- [21] O. M. Sleem, S. Leng, and A. Yener, “Age of information minimization in wireless powered stochastic energy harvesting networks,” in *Proc. CISS*, March 2020.
- [22] Z. Chen, N. Pappas, E. Bjornson, and E. G. Larsson, “Age of information in a multiple access channel with heterogeneous traffic and an energy harvesting node,” in *Proc. IEEE Infocom*, May 2019.
- [23] O. Ozel, “Timely status updating through intermittent sensing and transmission.” Available Online: arXiv:2001.01122.
- [24] G. Stamatakis, N. Pappas, and A. Traganitis, “Control of status updates for energy harvesting devices that monitor processes with alarms.” Available Online: arXiv:1907.03826.
- [25] J. Yang and S. Ulukus, “Optimal packet scheduling in an energy harvesting communication system,” *IEEE Trans. Commun.*, vol. 60, pp. 220–230, January 2012.

ProQuest Number: 28548749

INFORMATION TO ALL USERS

The quality and completeness of this reproduction is dependent on the quality and completeness of the copy made available to ProQuest.



Distributed by ProQuest LLC (2021).

Copyright of the Dissertation is held by the Author unless otherwise noted.

This work may be used in accordance with the terms of the Creative Commons license or other rights statement, as indicated in the copyright statement or in the metadata associated with this work. Unless otherwise specified in the copyright statement or the metadata, all rights are reserved by the copyright holder.

This work is protected against unauthorized copying under Title 17, United States Code and other applicable copyright laws.

Microform Edition where available © ProQuest LLC. No reproduction or digitization of the Microform Edition is authorized without permission of ProQuest LLC.

ProQuest LLC  
789 East Eisenhower Parkway  
P.O. Box 1346  
Ann Arbor, MI 48106 - 1346 USA